Research Article

Sustainable Backup Power Supply of a Hospital by Designing a Hybrid Renewable Energy System

Setare Peirow, Fateme Razi Astaraei *, Amir Ali Saifoddin Asl, Hossein Yousefi

Department of Renewable Energies and Environment, Faculty of New Sciences and Technologies, University of Tehran, P. O. Box: 14399-56191, Tehran, Tehran, Iran.

ABSTRACT

The issue of power supply in hospitals is of special importance because of its direct effect on people's health conditions and vital treatment and care measures. Hospitals are among buildings with high energy consumption. The possibility of using renewable sources in their energy supply is one of the issues and challenges that specialists encounter. This paper discusses the possibility of installing a small solar power generation unit on a hospital rooftop to improve the quality of power supply systems. The case study is a hospital located in Tehran, Iran. For this purpose, the hospital energy system was modeled with the Design-Builder software. The obtained results were validated based on the actual consumption of the model specified in the hospital energy bills. According to the modeling step results, the annual consumption of the current energy system was 3.08 GWh of electricity and 4.23 GWh of gas. In the second step, a renewable power generation unit consisting of photovoltaic panels and battery was designed for the hospital's roof using PVsyst software. The designed power generation unit could produce 132 MWh of solar energy per year, of which 85 MWh may be sold to the main grid. The techno-economic and environmental feasibility study for the proposed system was performed using HOMER Pro software. The evaluation results revealed that considering the 20-year lifetime of the project, the proposed system achieved a lower energy cost and lower net present cost than the current system. Environmental assessment of the model by considering emission penalty indicated that the proposed system emitted fewer pollutant gases into the environment than the current system. Sensitivity analysis was also applied to investigate the effect of discounting and diesel fuel price variation on the system's energy cost. According to the results, a 4 % increase in the discount rate leads to a 14 % growth in the cost of energy for the project. Also, there was a direct relation between enhancement of the expected inflation rate and raising the net present cost of the project.

1. INTRODUCTION

Hospitals are considered one of the main energy consumers in building sectors. Since hospitals and health centers constitute an energy-intensive group of buildings that must operate 24 h and 365 days a year, uninterrupted energy access is crucial for them [1, 2].

The issue of energy supply in hospitals is of special importance because of its direct effect on people's health conditions and vital treatment and care measures [3]. The energy-related issues have not received enough attention in constructing most of the existing hospitals [4]. Over the past few decades, hospitals have been designed and constructed only to meet required health standards, neglecting the environmental effect of energy systems due to the low cost of energy and disregarding the economic and environmental sustainability of human activities [5].

Since electricity consumption is higher in hospitals than in other buildings, renewable resources are a suitable option to employ to meet their electricity requirements [6]. On the other hand, including these resources in the energy basket of the healthcare sector facilitates sustainable energy development [7].

Considering the potential of solar energy in most parts of Iran and the incentives offered by the energy ministry to produce solar power for hospitals, a solar power generation unit is a suitable option to improve the power system. Also, generated solar power may be sold to the main network. Accurate sizing and quality equipment selection according to the climatic region are essential in order to reduce the probability of system failure [8].

2. EXPERIMENTAL

Different studies have been published with different viewpoints on the case of power supply in hospitals. Isa et al. (2016) evaluated the possibility of developing a combined

heat and power generation system for a Malaysian hospital [9]. The proposed cogeneration system included grid-connected photovoltaic, fuel cell, and battery. The simulation result indicated that the proposed cogeneration system had the lowest total net present cost, levelized cost of energy, and operating cost. Biglia et al. (2017) also performed a techno-economic feasibility analysis of CHP[1] systems in large hospitals through the Energy Hub method. Integration of a CHP system (internal combustion engine) into a multi-purpose energy system of the hospital has been studied since cogeneration is recognized as one of the most effective ways to convert energy. The proposed model is a valuable tool for examining potential energy and economic savings and for designing and optimizing every kind of multi-energy system of generic buildings, including hospitals [10].

Lagrange et al. (2020) studied different cases that required the use of renewable energies besides diesel generators and energy storage systems to increase the resilience of a microgrid so as to feed critical facilities of a hospital. The work aimed to quantify the benefits provided by an improvement of the energy resilience that could be achieved by installing a microgrid at a hospital fed by renewable energy sources [11]. Jahangir et al. and Dursan et al. (2021) also discussed the possibility of implementing hybrid renewable energy systems to supply the power demand for a hospital by making a comparison between techno-economic-environmental parameters [1, 12].

Shabnam Vaziri and Babak Rezaee et al. [13] tasted the PV[2]/WT[3]/Grid model for a hospital in Iran. According to the results, hospital costs were reduced by 2.7 %, while hospital loads decreased during peak hours. Their model discovered a tradeoff between costs and satisfaction of patients and medical practitioners. Another study by Andrea Franco and Marjan Shaker et al. [14] in Switzerland reported that a hybrid configuration consisting of renewable energy resources, a battery, and a diesel generator was the best option for medium-to-large healthcare facilities, especially for those in off-grid settings. Table 1 tabulates a list of the mentioned articles with the key subject and final result. The main difference between recent articles and current study is also addressed in the Table 1.

The main challenge of recent studies has been complete and accurate modeling of the hospital energy system as a large-scale and complex structure, which need all of the building plans, section usage, and details of its energy system. So far, few studies have been conducted on simulating the energy system of a complicated hospital. Furthermore, identification of the environmental benefits of integrating the energy system of hospitals as a complex structure with renewable energies was not considered in recent studies.

Iran is a vast country with many hospitals, health centers, and medical buildings. Most of the energy needs of these areas are met by fossil fuels which impose environmental impacts on the country. The grid is typically used to meet the load demand of hospitals, and diesel generator is often implemented as backup for power supply. Using renewable energies in the power supply system is an appropriate choice that may help improve the quality of the power supply system and have an influential role in reducing pollution in medical buildings.

This paper proposed photovoltaic modules with batteries to integrate with the power supply system. The hybridization with the solar system and battery enhances the energy security in the model. To this end, using the solar power plant with a weak network support strategy was proposed. First, the hospital's energy system was modeled using Design-Builder Software (version 6.1.0.006). The software was applied to model the building from different aspects, namely building physics (construction materials), building architecture, cooling and heating systems, and lighting systems [18]. Second, a hybrid energy system consisting of photovoltaic modules and batteries was modeled with PVsyst software (version 6.8.1) to add to the previous backup power supply consisting of only a diesel generator. Finally, a techno-economic and environmental evaluation of the proposed system was performed to justify the project's feasibility. HOMER Pro software was used for this section and sensitivity analysis was applied to indicate the effect of financial factors on the system's cost variation.

3. METHOD

3.1. Methodology

In this research, the hospital energy system was modeled using Design-Builder software (version 6.1.0.006), which is convenient for modeling different aspects of the building. The software can utilize the climate data files of different cities to calculate the energy input, consumption, and losses for the region the building is located in. The modeling engine in the software is EnergyPlus developed by American Energy Department and is considered a highly accurate and capable software product. System modeling in EnergyPlus is performed based on the following computational relationships.

3.2. Basis for the zone and air system integration

The basis for the zone and air system integration is to formulate energy and moisture balances for the zone air and solve the resulting ordinary differential equations using a predictor-corrector approach. The formulation of the solution scheme starts with a heat balance on the zone air tabulated in Table 2.

Air systems provide hot or cold air to the zones to meet heating or cooling loads. The system energy provided to the zone, $\dot{Q}_{sys}$, can thus be formulated from the difference between the supply air enthalpy and the enthalpy of the air leaving the zone as in Equation (2). This equation assumes that the zone supply air mass flow rate is equal to the sum of the air flow rates leaving the zone through the system return air plenum and being exhausted directly from the zone. Both air streams exit the zone at the zone mean air temperature.

The sum of zone loads and air system output now equals the change in energy stored in the zone. Typically, the capacitance C_z would be that of the zone air only. However, thermal masses assumed to be in equilibrium with the zone air could be included in this term. EnergyPlus provides three different solution algorithms to solve the zone air energy and moisture balance equations.

3.3. Conduction transfer function module

The most basic time series solution is the response factor equation that relates the flux on one surface of an element to

---

[1] Combined Heat and Power

[2] Photovoltaic

[3] Wind Turbine

an infinite series of temperature histories on both sides, as   shown by Equation (3) in Table 3.

Table 1. Summary of literature review

Reference	Subject	Result	Difference with present study
[9]	Possibility of developing a combined heat and power generation system for a Malaysian hospital.	The proposed cogeneration system has the lowest total net present cost, levelized cost of energy, and operating cost.	Type of hybrid system proposed for the hospital differs from the one in the current study.
[10]	Techno-economic feasibility analysis of CHP systems in large hospitals.	The proposed model was a useful tool to examine potential energy and economic savings and design and to optimize every multi-energy system.	Renewable energies for the hospital power supply were not addressed in this study.
[11]	Use of renewable energies in addition to diesel generators and energy storage systems with the aim of increasing the resilience of a micro grid feeding critical facilities of a hospital.	With high solar resources and for the electricity tariff studied, the addition of solar PV makes it possible to increase the resilience of a microgrid in the event of power outages.	This study focused on the resiliency of microgrids, while the current article deals with the techno-economic and environmental assessment of the hybrid system.
[12-15]	The possibility of implementing hybrid renewable energy systems to supply the power demand for a hospital.	The proposed hybrid system has the lowest total net present cost, levelized cost of energy, and operating cost.	Environmental evaluation and sensitivity analysis were not addressed in these studies.

Table 2. Heat balance in the zone air equation [16]

Zone air heat balance relations	Equations No.
$$C_z \frac{dT_z}{dT} = \sum_{i=1}^{Ns1} \dot{Q}_i + \sum_{i=1}^{N_{surface}} h_i A_i (T_{si} - T_z) + \sum_{i=1}^{N_{zone}} \dot{m} C_p (T_{zi} - T_z) + \dot{m}_{inf} C_p (T_\infty - T_z) + \dot{Q}_{sys}$$	(1)
$$\dot{Q}_{sys} = \dot{m}_{sys} C_p (T_{sup} - T_z)$$	(2)
$C_z \frac{dT_z}{dT}$ = energy stored in zone air ($C_z = \rho_{air} C_p CT$; ρ_{air} = zone air density; C_p = zone air specific heat; CT = sensible heat capacity multiplier)	
$\sum_{i=1}^{Ns1} \dot{Q}_i$= sum of the internal convective loads $\\$ $\sum_{i=1}^{N_{surface}} h_i A_i (T_{si} - T_z)$ = convective heat transfer from the zone surfaces $\\$ $\sum_{i=1}^{N_{zone}} \dot{m} C_p (T_{zi} - T_z)$= heat transfer due to interzone air mixing $\\$ $\dot{m}_{inf} C_p (T_\infty - T_z)$ = heat transfer due to infiltration of outside air $\\$ $\dot{Q}_{sys}$ = air systems output $\\$ T_{sup}= supply air temperature	

Table 3. The equations of change and rates for anode and cathode [16]

Conduction transfer relations	Equations No.
$$q''_{ko}(t) = \sum_{j=0}^{\infty} X_j T_{o,t-j\delta} - \sum_{j=0}^{\infty} Y_j T_{o,t-j\delta}$$	(3)
$$q''_{ki}(t) = -Z_0 T_{i,t} - \sum_{j=1}^{nz} Z_j T_{i,t-j\delta} + Y_0 T_{0,t} + \sum_{j=1}^{nz} Y_j T_{0,t-j\delta} + \sum_{j=1}^{nq} \Phi_j q''_{ki,t-j\delta}$$	(4)
$$q''_{ko}(t) = -Y_0 T_{i,t} - \sum_{j=1}^{nz} Y T_{i,t-j\delta} + X_o T_{0,t} + \sum_{j=1}^{nz} X_j T_{0,t-j\delta} + \sum_{j=1}^{nq} \Phi_j q''_{ko,t-j\delta}$$	(5)
In Eq. 3, "q" is heat flux, T temperature, i the inside of the building element, o the outside of the building element, t the current time step, and X and Y the response factors.	
In Eqs 4 and 5, the outside heat flux is: $q''=q/A$ $\\$ X_j = Outside CTF coefficient, j= 0, 1, nz. $\\$ Y_j = Cross CTF coefficient, j= 0, 1, nz. $\\$ Z_j = Inside CTF coefficient, j= 0, 1, nz. $\\$ Φ_j = Flux CTF coefficient, j = 0, 1, nz. $\\$ T_i = Inside face temperature $\\$ T_o = Outside face temperature $\\$ q''_{ko}= Conduction heat flux on the outside face $\\$ q''_{ki}= Conduction heat flux on the inside face	

While the terms in the series decay fairly rapidly in most cases, the infinite number of terms needed for an exact response factor solution makes it less than desirable. Fortunately, the similarity of higher-order terms can be used to replace them with flux history terms. The new solution contains elements that are called Conduction Transfer Functions (CTFs). The basic form of a conduction transfer function solution is shown by Equations 4 and 5 in Table 3.

The subscript following the comma indicates the period for the quantity in terms of the time step δ. Note that the first terms in the series (those with subscript 0) have been separated from the rest in order to facilitate the resolution at the current temperature in the solution scheme. These equations state that the heat flux at either face of the surface of any generic building element is linearly related to the current and some of the previous temperatures on both the interior and exterior surfaces, as well as some of the previous flux values on the interior surface.

The final CTF solution form reveals why it is so elegant and powerful. The conduction heat transfer through an element can be calculated with a single, relatively simple, linear equation with constant coefficients. The coefficients (CTFs) in the equation are constants that only need to be determined once for each construction type. The only data required for storage include the CTF and a limited number of temperature and flux terms. The formulation is valid for any surface type and does not require the calculation or storage of element interior temperatures.

Additional information on modeling details of different parts of the system and the formulation used is given in the reference [16].

3.4. Simulation in Design-Builder

In order to start modeling, first, the Three-Dimansional (3D) model of the building was drawn in the Design-Builder software. The 3D plan models were generated using the model files, which are in the format of AutoCAD plans. The plan includes the building, its orientation, how doors and windows are built-in, and also the different zones on the floors. Figure 1 shows a view of the building floors and plans in Design-Builder.

Ghiasi specialized hospital in the south-western part of Tehran was selected for this study. This hospital has a total area of 17300 square meters and 16000 meters of space on all the floors. Different diagnostic and therapeutic departments such as laboratories, Computed Tomography (CT) scans, ophthalmology, emergency unit, pharmacy, etc. are located on the ground floor. In contrast, hospital wards, operation rooms, Coronary Care Unit (CCU) and Intensive Care Unit (ICU) departments are located on the higher floors.
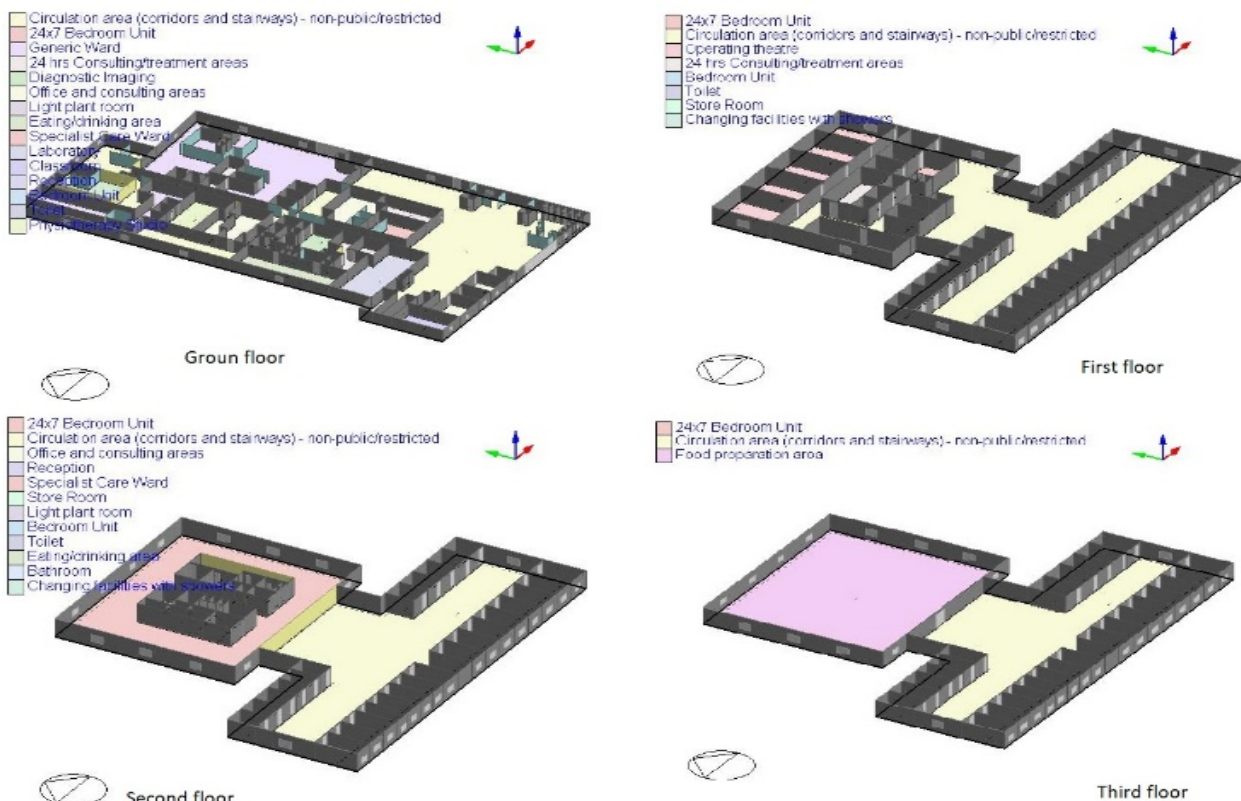

Figure 1. Plan of Hospital floors

Figure 2 shows an aerial photograph of the hospital. Considering the solar energy potential in Tehran, the hospital's roof, which has an area of about 900 square meters, is a suitable place to install solar panels.

After designing the building plan, the energy system's data and installation information were entered into the software. Some of these data are listed in Table 4.

3.5. Design of a small solar power generation unit on the roof of the hospital

The current energy system of the hospital operates using fossil resources. The power demand is supported by the main grid and diesel generators are installed as the backup system. Due to the great potential of solar power generation in Tehran [17], the hospital's energy system is recommended to combine with

the solar energy system. Iran is located between 25° and 40° north latitudes in one of the earth's regions with suitable sun radiation. The solar average radiation intensity in Iran is higher than the global average, and more than 280 sunny days have been recorded in more than 90 % of Iranian lands [18]. Figure 3 shows the average monthly radiation in Tehran.
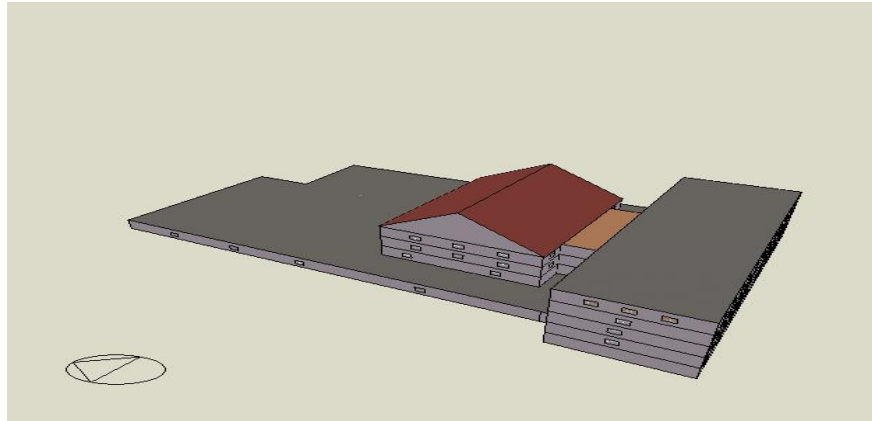
Figure 2. Aerial photograph of the hospital (Map designed in Design-Builder)

Table 4. Input data in Design-Builder

Input data	Value entered in Design-Builder
Geographical location of hospital	Tehran-Mehrabad
Latitude and longitude	35.69° N, 51.31° E
Building plan	3D design is produced by calling the DXF file
Location of doors, windows, and building spaces	Based on the building plans
Building use	The use of each space is entered (e.g., laboratory, ward, clinic, etc.)
Frequency of occupants' presence in each space	It is determined according to the use of each space
Comfort temperature in winter	22-25 °C
Comfort temperature in summer	25-28 °C
Hot water consumption	It is determined according to the use of each space
Energy consumption for computers, office supplies, etc.	It is determined according to the use of each space and the time schedule
Energy required for cooking	The required energy and its source are determined for the food-cooking space (200 W/m^2)
Building wall materials and their thickness	Brick walls of the thickness of 40 cm (based on the intended building features)
Building façade	Cement façade of thickness 5 cm
Quality of sealing	Medium
Type of window	Transparent and double-glazed
Type of lamps	Low standard (15 W/m^2)
Type of air-conditioning system	Fan coil unit (4 pipes), Air-cooled chiller
COP of cooling system	2
COP of heating system	0.85
Hot water supply system	Boiler with 85 % efficiency
Energy source of cooling system	Electricity
Energy source of heating system	Natural gas
Energy source of hot water supply	Natural gas
Energy source for cooking	Natural gas
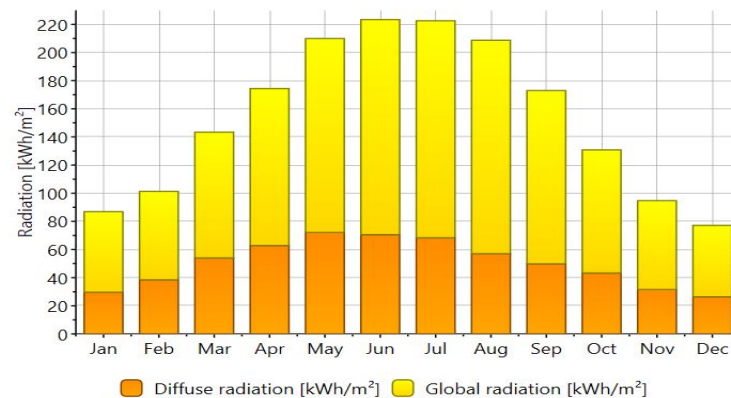
Figure 3. Monthly diffuse and global radiation in Tehran (Meteonorm output)

The windows, building facades, and roof can be employed for solar power generation in the model. To generate power from solar energy, the type of glasses and materials used in the façade must be replaced, which is a costly and unavailable option. The easiest way to produce solar power is to install photovoltaic panels on the roof of the hospital.

The Photovoltaic (PV) panels and the installation process on the rooftop were modeled using the PVsyst software (version 6.8.1). Design parameters such as module orientation, near shading, and inter-row spacing were evaluated.

PVsyst is a versatile software product for designing solar photovoltaic panels that can help the operator accurately design and simulate a power plant by utilizing a package of built-in libraries and the desired brands in any configuration. It also enables the user to add new equipment to the software environment, manipulate the system to extract the highest efficiency from the solar power plant, and select the best configuration by calculating the effect of different parameters on the solar power plant.

Shadow analysis is one of the essential steps in the phase of solar energy system design or analysis. In solar cells, it is important to analyze shading caused by surrounding objects and/or vegetation [19]. The shaded solar cell acts as a power load instead of a power producer. The reverse voltage exceeds the breakdown voltage that leads to hotspot formation. In this study, shading analysis is done in the PVsyst workspace and the final design consists of a possible minimum shadow effect.

In this case, considering the total available space area for use as 900 m², 80 kilowatts of solar panel capacity has been selected to be installed on the rooftop. The type of selected panels is 250 W from the Sharp brand. To size a solar PV array, cells are assembled in the form of a series-parallel configuration for requisite energy.

To compensate for emergencies and electricity deficiency from the grid, the Weak Grid and Islanding mode strategies in PVsyst were suggested for the installation of PV panels on the rooftop.

The national electricity grid meets most of the hospital's electricity demand. However, due to the unavailability of the grid during network disruption, other electricity resources are needed to support the system.

Grid reliability is defined in the model by three parameters. These items are mean outage frequency, mean repair time, and repair time variability, which are quantified in Table 5. These items are considered based on the reliability of the electricity supplier network in the study. The electricity cut-off profile of the hospital is illustrated based on the field research by visiting the considered hospital and technical assistants' reported statistics about the number of annual electricity cutoffs. The times of these cut-offs and repairing networks are determined according to obtained statistics from the hospital in one year. By specifying these items, a random chart of grid outages through the year is generated by the software (Figure 4). Most of these outages occur during the day because of the pick power demand and more loads are imposed on the network during the day.

Table 5. Grid reliability parameters

Parameter	Unit	Value
Mean outage frequency	1/year	60
Mean repair time	h	0.5
Repair time variability	%	30
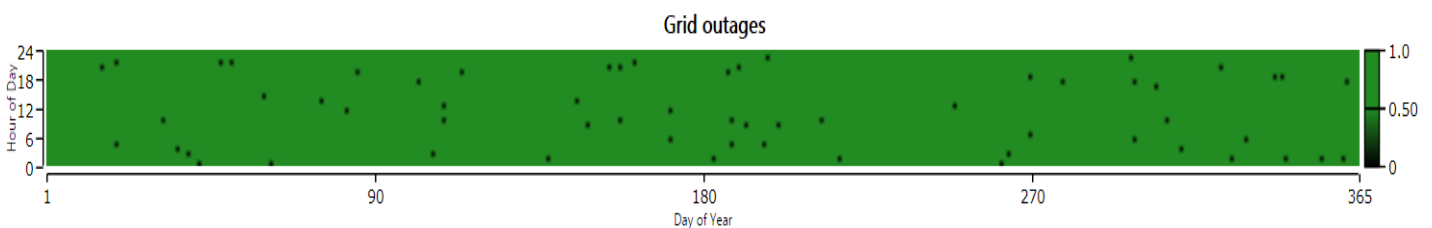
Figure 4. Random graph of grid outages through the year

The Weak Grid strategy uses batteries resource to prevent electricity deficiency. In this scenario, batteries will be used to cover a self-consumption load profile. However, the battery source depletion will be limited to a certain threshold, which allows the load profile to stay in the safe region in case of possible interruptions. When there is an interruption, the energy saved in the battery system is allowed to exceed the limits and reach depletion.

To reach this goal, the selected battery for this project, which is from the Tesla brand, has a nominal capacity of 268 Ah. Self-consumption load profile was considered to be 10 kW. This load is enough to cover the power demand of hospital emergency corridors. Therefore, a reliable electricity supplier was defined for emergency corridors to promote hospital security in case of unexpected events.

When there is a network failure, there should be a mechanical switch for the physical disruption of the network from the connected mode. In this condition, the system will operate in islanding mode and the battery inverter supplies all the energy required by the consumer. In the connected mode, the user AC[1] circuit is directly connected to the grid; this gives the network the possibility of injecting additional solar energy, even though this is not always allowed by the network administrator. Figure 5 shows a schematic of the proposed network.

---

[1] Alternating Current
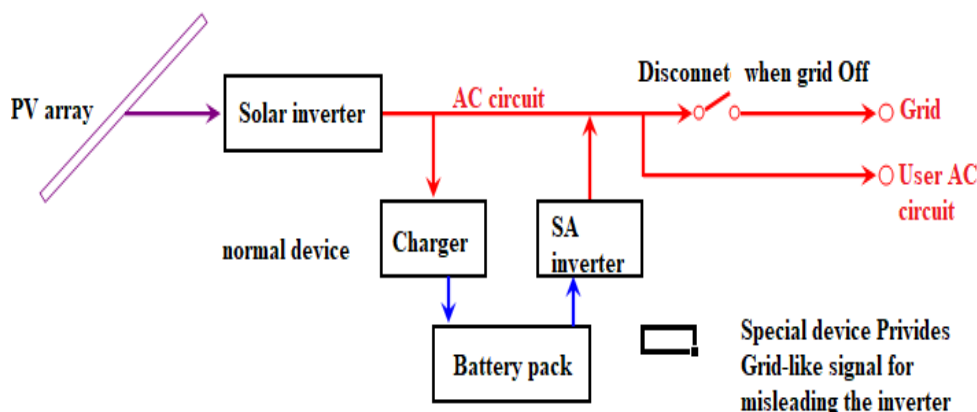
Figure 5. Proposed configuration for supporting the weak network and islanding mode

3.6. Designed model in PVsyst

The system comprises 324 panels with a total area of 532 m². In the designed model in PVsyst, there are 12 cells connected in series and 27 modules connected in parallel. The panels were installed in a fixed position and at an angle of 33° relative to the horizon. The total number of 9 unit inverters from the SMA brand were installed to convert solar power. Table 6 presents additional information about the plant.

Table 6. Input data in PVsyst

System type	Sheds on ground
Tilt 33°	Azimuth 0°
Number of sheds: 27	Sheds spacing: 6.7 m
Collector width: 3.36 m	Ground cover ratio (GCR): 50.1%
Charging strategy	When excess solar power is available
Discharging strategy	As soon as power is needed

Table 7 represents the specifications of the solar panel and the inverters, while Table 8 shows the properties of the batteries. Table 9 shows the details of the place where the power plant will be constructed. Figure 6 shows the configuration of installed panels on the hospital rooftop.

A suitable controller is responsible for managing the energy flux all the time. There are multiple scenarios in this case. If the solar energy is sufficient for the user, the excess energy would be used to charge the batteries. In the case of fully charged batteries, the rest of the energy will be injected into the grid. In case of insufficient sun energy or during the nights, the energy demand will be supplied by the batteries.

The current backup system of the model comprises a diesel generator with a capacity of 1000 kW.

**Table 7.** Specifications of panel and inverter installed at the power plant

Specification	Inverter	Panel
Brand	SMA	Sharp
Capacity	7.7 kW	250 Wp
Voltage	300-480 V	26 V
Manufacturing technology	LF-TR	Si-Poly
Model	Sunny boy 8000 U-240	ND-RC250
Year manufacture	2010	2016

Table 8. Battery specifications

Type	Lithium-Ion
Brand	Tesla
Model	Powerwall 2
Voltage	50.4 V
Nominal capacity	268 Ah
Stored energy (DOD 80 %)	10.8 kWh
Weight	125 Kg
Total stored energy during battery life	10186 MWh
Global capacity	804 Ah

Table 9. Geographical location

Country	Iran
Geographical site	Shahrak-e Farhangian
Latitude	35.70° N
Longitude	51.28° E
Altitude	1230 m
Albedo	0.2
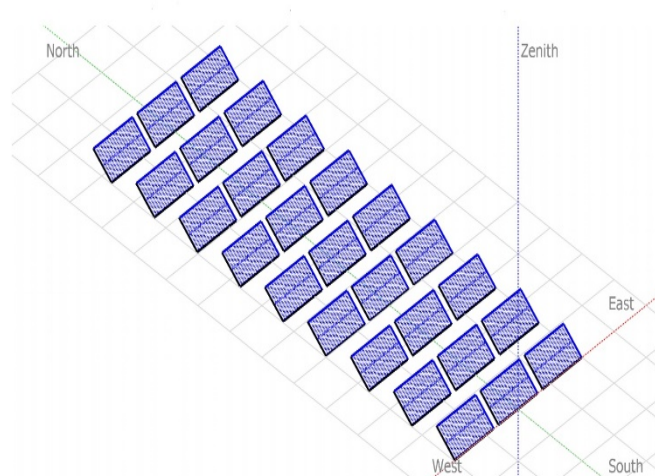
Figure 6. Arrangement of the panels installed on the hospital ceiling

3.7. Economic and environmental analysis

The economic and environmental analysis of the suggested system was performed using HOMER Pro software. HOMER is known as wide-ranging software for the investigation and development of hybrid sources. This software is made and developed by US National Renewable Energy Laboratory

(NREL). Its name stands for Hybrid Optimization Model for Electrical Renewable. This software (version 3.14.2) is ready to detect the most cost-effective system for a given load by considering incident solar radiation, electrical demand profile, and equipment properties.

The energy load demand of the hospital is obtained from the Design-Builder output. Thus, the monthly and daily electrical output of the Design-Builder is used as the input data for HOMER pro software. Figure 7 shows the average monthly load of the hospital.
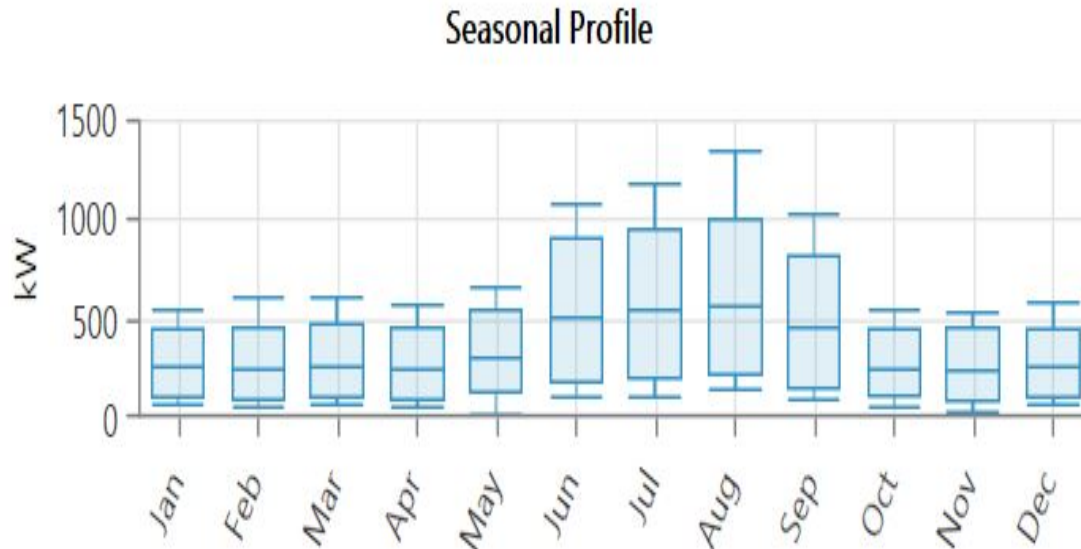

Figure 7. Monthly average load profile for the hospital

3.7.1. Calculating the cost of the system

The system designed in the PVsyst includes photovoltaic panels and a battery in the grid-connected mode. A 700 kW diesel generator is also connected to the power supply system to support the power supply in case of an emergency. Thus, the system consists of photovoltaic panels (sharp ND-250QCS), an inverter, a battery (Tesla Powerball 2), and a diesel generator (Generic Medium Genset). In order to calculate the total cost of the system, techno-economic specifications of components should be entered into HOMER software. Tables 10-13 show technical factors and cost assumptions of the system's components.

Table 10. Technical parameters of solar PV array and cost assumptions

Parameter	Unit	Value
Nominal max. power	W	5000
Capital cost	$/kW	1000
Replacement cost	$/kW	1000
Operation and maintenance cost	$/kW/yr	10
Lifetime	Years	20
Efficiency	%	15.3

Table 11. Technical parameters and cost assumptions for the battery

Parameter	Unit	Value
Nominal voltage	volt	220
nominal capacity	Ah	60
maximum charge current	A	31.8
round-trip efficiency	%	90
capital cost	$	65000
replacement cost	$	65000
operation and maintenance cost	$/year	600
life time throughput	kWh	67500
life time	years	10

Table 12. Techno-economic parameters of the converter

Parameter	Unit	Value
Capital cost	$/kW	500
Replacement cost	$/kW	500
Operation and maintenance cost	$/kW/yr	10
lifetime	Years	20
Inverter efficiency	%	95
Rectifier efficiency	%	85

Table 13. Technical parameters and cost assumptions for diesel generator

Parameter	Unit	Value
Capital cost	$/kW	900
Replacement cost	$/kW	700
Operation and maintenance cost	$/kW/yr	0.02
lifetime	Hours	15000
Rated capacity	kW	1000

The economic factors consisting of the inflation rate, the discount rate, the project's life time, and diesel fuel price are the essential software entries for the economic optimization. These factors are tabulated in Table 14.

Table 14. Financial input factors for simulation of hybrid energy systems

Input factor	Value	Ref
Inflation rate (%)	15	[20]
Discount rate (%)	18	[20]
Life time of the project (years)	20	
Diesel fuel price ($/L)	0.1	[15]

Figure 8 specifies the yearly electricity prices and network power purchase rate in Iran, specified by the government. Based on the mentioned rates, energy prices differ in cold and

hot months. On the other hand, while the demand rate is high, the electricity price is twice the low demand rate [21].
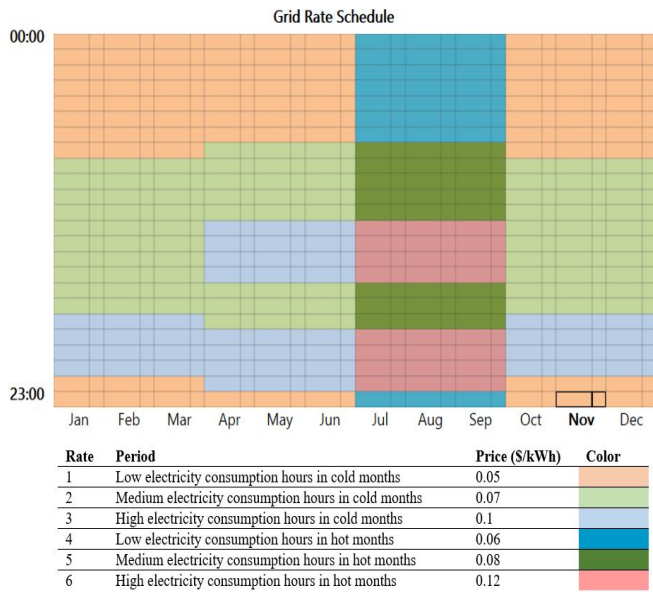

Rate	Period	Price ($/kWh)	Color
1	Low electricity consumption hours in cold months	0.05	
2	Medium electricity consumption hours in cold months	0.07	
3	High electricity consumption hours in cold months	0.1	
4	Low electricity consumption hours in hot months	0.06	
5	Medium electricity consumption hours in hot months	0.08	
6	High electricity consumption hours in hot months	0.12	

Figure 8. Grid annual electricity tariffs in Iran [21]

Annual system total cost is dependent on two fundamental economic factors: NPC and COE. NPC defines the net present cost of the system, while COE describes the cost of energy of the model. NPC comprises the annual cost of components consisting of capital cost, operation and maintenance (O&M) cost, and replacement cost, excluding any miscellaneous expenses such as CO_2 emissions [22, 23]. COE is the cost of enegy of the system which means the amount of cost imposed on the system to produce each kilowatt of energy. In fact, NPC has a mathematical concept, while COE is kind of arbitrary [23]. Hence, NPC is more dependable as an economic parameter and is calculated using the following equation in Table 15.

Table 15. Economic parameters and related equations [23]

Cost relations	Equations No.
$NPC = \dfrac{C_T}{CRF\,(i,n)}$	(6)
$C_T = C_{acap} + \sum\limits_{j=1}^{m} C_{OM,j} + C_f + \sum\limits_{j=1}^{m} C_{R,j}$	(7)
$C_{acap} = C_{cap} \times CRF$	(8)
$CRF(i,n) = \dfrac{i(1+i)^n}{(1+i)^n - 1}$	(9)
In Eq. 6, C_T is the total annualized cost ($/year), i the annual real interest rate (%), n the project's lifetime, and CRF the capital recovery factor.	
In Eq. 7, C_{acap} is the annualized capital cost of each component and C_{cap} is the initial capital cost of a component defined as the total installed cost of that component at the beginning of the project. m=The number of all devices in the system. $C_{OM,j}$= The annual operation and maintenance (O&M) cost for the jth component of the system. C_f =The total annual fuel cost. $C_{R,j}$ = The annualized replacement cost for the jth component of the system.	

3.7.2. Evaluating environmental impacts

For the sake of environmental impact analysis of the proposed system, the amounts of emitted greenhouse gases should be detected. Considering emission penalties for various industries is a common policy that helps reduce and control harmful emissions. Therefore, for each ton of emissions, the penalty must be paid to the government by factory owners. The amounts of considerable emissions for Iran's power plants are shown in Table 16. CO_2 with an emission content of 660.65 g/kWh has the maximum contribution. Therefore, the higher values of penalty are related to more harmful emissions, which lead to more dangerous circumstances for the environment and human health. Since Particulate Matter (PM) has the most severe impact on the whole environment, it owes the most considerable value of penalty (1228.60 $/ton) [20].

Table 16. The emission content of Iran's power plants [20]

Kind of emission	Value (g/kWh)	Penalty of emission ($/ton)
Carbon Dioxide (CO_2)	660.65	2.86
Carbon Monoxide (CO)	0.62	54
Unburned Hydrocarbons (UHC)	180.18	60
Nitrogen Oxides (NO_X)	2.38	171.5
Sulfur Dioxide (SO_2)	1.66	521.5
Particulate Matter (PM)	0.12	1228.6

HOMER software estimates the release rate of each configuration. Therefore, the environmental state of the proposed model can be evaluated by calculating its pollution level and compared with the current model.

4. RESULTS AND DISCUSSION

4.1. Basic Model

The energy system modeling outputs for Ghiasi hospital during a one-year[1] simulation in Design-Builder are as follows. The annual electricity consumption is 3.08 GWh and the annual gas consumption is 4.23 GWh. Natural gas and electrical energy account for 58 % and 42 % of the annual consumption basket, respectively (Figure 9). Figure 10 shows the yearly power required for cooling and heating systems, hot water production, lighting, electrical equipment and devices, and cooking. The building heating system and electrical equipment, with 1.91 GWh and 0.86 GWh energy usage, have the highest and lowest contribution, respectively. Figure 11 illustrates the contribution of each different consumer to the annual energy consumption of the hospital. The yearly heating by 26 % of the energy required is the highest annual consumption.
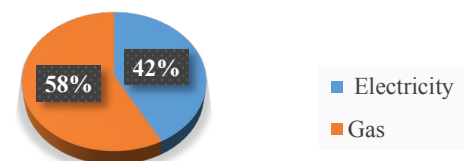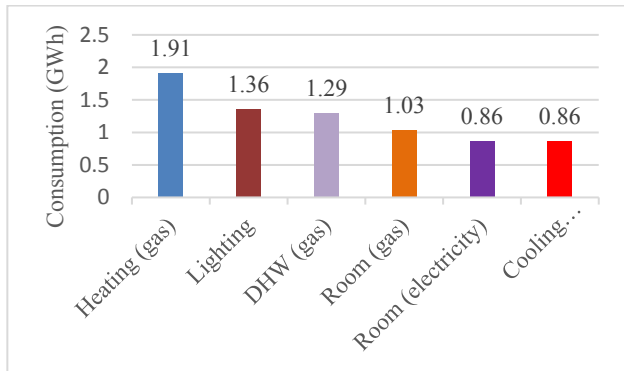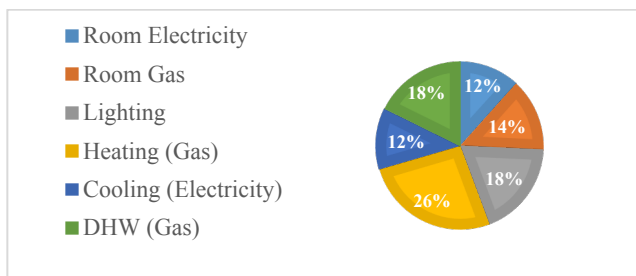

Figure 9. Circular diagram of gas and electricity contribution to annual energy consumption (obtained by Design-Builder)

---

[1] The year of running simulation was 2020.

Figure 10. Energy consumption in the hospital (obtained by Design-Builder)

Figure 11. Contribution of different consumers to the annual energy consumption (DHW stands for district hot water)

4.2. Validation of the model

In order to validate the obtained results and compare them with the energy system performance in the hospital, the outputs are represented in a monthly manner according to the date of the hospital's utility bills, making it easy to compare the amount of gas and electricity consumption of the model with the existing system. Therefore, the electricity consumption intensity of the model has little difference from the hospital's electricity bill, and the modeling error is less than 10 %, which proves the accuracy of the modeling process.

Electricity consumption

Table 17 demonstrates data on the hospital's electricity bill (2020) and the model's power consumption amount. According to this table, the electricity consumption of specified periods based on model output slightly differs from energy bills (Figure 12). The model error is recorded at each measuring interval. According to this table, the model's power consumption is 3.045 GWh during the simulation period, while the actual consumption based on the electricity bill is about 3.012 GWh. Therefore, the modeling error is 1 %, which is an acceptable value and represents the accuracy of the modeling process.

Table 17. Electricity bills data and comparison with model outputs

Period number	length of the billing cycle (date)	Duration	Actual consumption (MWh)	Model consumption (MWh)	Relative error (%)
1	13 Feb.-9 Apr.	55	379.2	344	9
2	9 Apr.-8 May	29	192	181	5
3	8 May-9 Jun.	32	352	376	6
4	9 Jun.-12 Jul.	33	448	455	1
5	12 Jul.-6 Aug.	25	374.4	386	3
6	6 Aug.-6 Sep.	31	427.2	450	5
7	6 Sep.-4 Oct.	28	353	380	7
8	4 Oct.-3 Nov.	30	245.4	263	3
9	3 Nov.-7 Dec.	34	233.6	210	9
Total		297	3012.8	3054	1
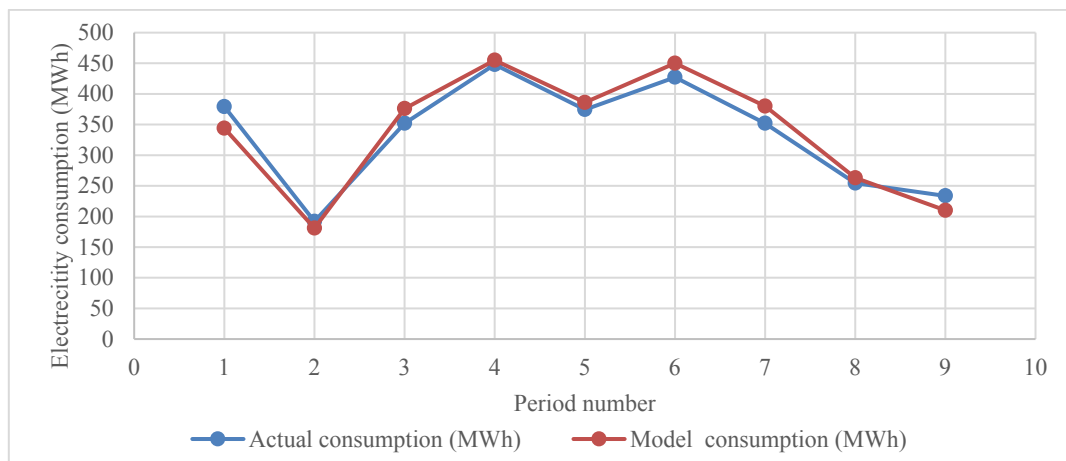
Figure 12. Electricity consumption of the specified periods based on model output and energy bill

4.3. Solar power unit

After entering the data required in PVsyst and running the simulation, the following results are obtained. Table 18 shows the monthly and annual power generated by panels. According to Table 7, 137.7 MWh can be generated by panels annually, and 87.6 MWh can be consumed to provide the self-consumed constant-profile electricity defined in the program (part of the lighting in the hospital corridors). The rest is either stored in a battery or sold to the network. According to the table, 85.56 of solar electricity is sold to the grid annually. Figure 13 displays monthly solar power production versus power injected into the grid. The difference between these two diagrams shows the amount of solar power consumed in the system. As shown in the figure, in summer, the power production reaches its maximum due to the greater intensity of sunlight in these months.

The output currents of the generated power on the panel surface are plotted in the Sanki diagram (Figure 13). Figure 14 also displays the monthly solar power production versus the power injected to grid. The difference between these two diagrams shows the amount of solar power consumed in the system. As shown in the figure, the amount of the power production in summer reaches its maximum, which is due to the greater intensity of sunlight in these months.
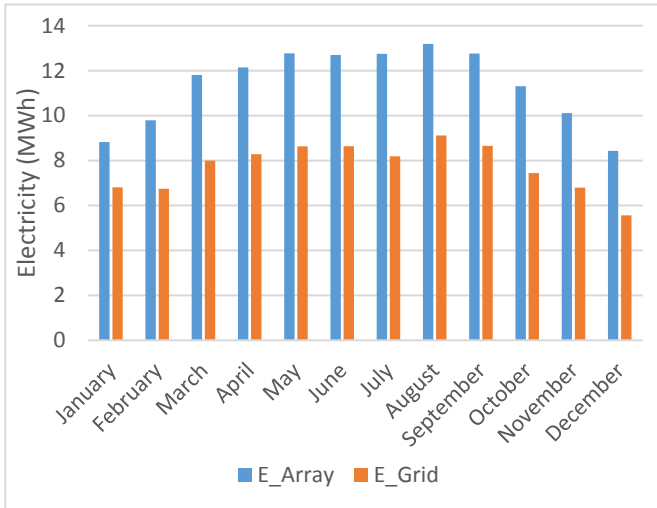
Figure 15 displays the performance ratio of the solar power plant in different months of the year. The performance ratio of the power plant is defined as the ratio of the modules' actual power on the panel surface to their rated capacity. The performance ratio is an index of the photovoltaic power plant quality; therefore, it is often described as a quality factor. The PR is expressed as a percentage and describes the relationship between the actual and theoretical energy output of the PV power plant. Figure 15 indicates that the power plant's the impact of increased temperature on the panel surface. The annual average of PR is 0.766.

Table 18. Monthly information on solar radiation and production (balances and results from PVsyst)

	GlobHor (kWh/m^2)	DiffHor (kWh/m^2)	T_Amb (°C)	GlobInc (kWh/m^2)	GlobEff (kWh/m^2)	EArray (MWh)	E_user (MWh)	E_Grid (MWh)	EFrGrid (MWh)	E_Miss (MWh)
January	85.8	24.76	4.30	142.5	135.0	8.82	7.44	6.805	4.804	0.10
February	99.1	37.37	7.33	138.3	131.8	9.79	6.720	6.745	4.100	0.08
March	140.8	49.27	12.99	172.0	163.9	11.81	7.44	7.995	4.282	0.00
April	171.4	73.08	17.67	180.9	170.4	12.14	7.20	8.280	3.753	0.14
May	207.1	68.06	23.31	196.8	185.5	12.77	7.44	8.633	3.759	0.13
June	221.7	69.55	28.38	201.2	189.6	12.70	7.20	8.639	3.611	0.03
July	220.2	75.92	31.32	205.0	193.0	12.75	7.44	8.188	3.729	0.02
August	206.3	68.04	30.82	211.1	199.7	13.19	4.44	9.118	3.862	0.02
September	170.8	52.81	26.08	199.4	189.8	12.76	7.20	8.649	3.846	0.11
October	125.7	40.58	20.45	171.3	163.7	11.31	7.44	7.44	4.404	0.08
November	93.9	30.69	11.73	148.7	141.0	10.11	7.20	6.795	4.426	0.09
December	76.1	25.56	6.05	128.4	121.0	8.43	7.44	5.558	5.021	0.06
Year	1820.9	615.69	18.43	2095.5	1984.5	137.57	87.600	92.849	49.598	0.860

GlobHor	Horizontal global irradiation	EArray	Effective energy at the output of the array
DiffHor	Horizontal diffuse irradiation	E_User	Energy supplied to the user
T_amb	Ambient temperature	E_Grid	Energy injected into the grid
GlobInc	Global incident in coll. Plane	EFrGrid	Energy from the grid
GlobEff	Effective Global, corr. for IAM and shading	E_Miss	Missing energy
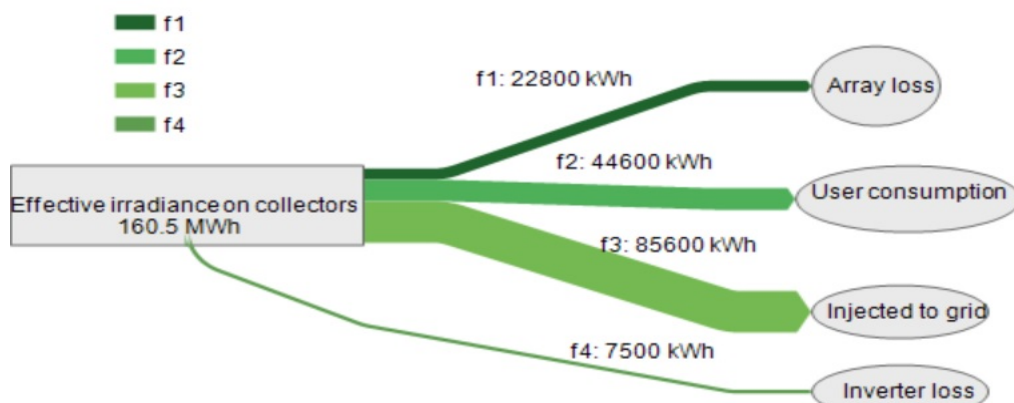
**Figure 13.** Sankey diagram of the electric current generated by collectors

Figure 14. Monthly solar power production (E_Array) versus power injected into the grid (E_Grid)
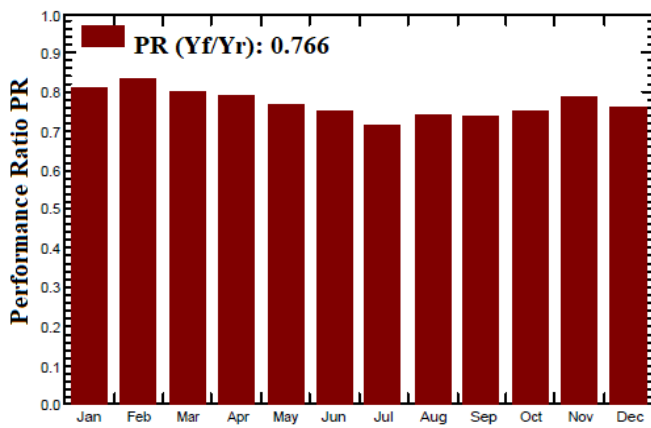
Figure 15. Performance ratio of the solar power plant in different months

Figure 16 shows the arrow loss diagram of the solar plant. As can be seen, from 1958 kWh of solar radiation energy that is incident on a square meter unit of panels with 15.9 % efficiency (in Standard Test Conditions (STC)), only 160.5 MWh can be produced in the rated condition (STC) on the array surface. 38 % of the energy generated is wasted by the loss of radiation associated with the irradiance level. These losses arise from the intrinsic behavior of the PV module since a certain amount of solar radiation is not absorbed in the morning and evening by the cells due to the insufficient space between two consecutive rows of solar cells, resulting in radiation losses. The second factor of energy loss is temperature. The cell efficiency decreases by increasing its temperature, which causes the loss of 10 % of the energy generated in the module. Other energy loss factors have a lower contribution, as shown in the figure. Finally, after deducting all the losses available, 137.7 MWh is generated at the panel level, of which 3.91 % is wasted by passing from the inverter, and 132.3 MWh can be achieved at the inverter outlet. This energy is used for recharging the battery, self-consumption constant profiles and injection into the main grid. When the battery is charging, 0.67 % of the generated energy is dissipated, while it is 0.96 % when the battery is filled as unused energy. Finally, 44.6 MWh is used to supply a constant electricity profile and 85.6 MWh is sold to the grid.

Figure 17 shows the Meteonorm horizon for the the power plant site. Blue lines indicate the tangential limits of the plane (i.e., when the sun rays are parallel to the plane). The solar radiation and PV output will change if local hills or mountains block the sunlight during some periods of the day; thus, the horizon profile helps achieve accurate output data. The horizon profile may be defined manually by a set of (Azimuth/Height) points in degrees. These may be from on-site measurements (using land-surveyors instruments like compass and clinometer). They can also be imported from several sources. In this project, the Meteonorm software produces horizon profiles imported in PVsyst.
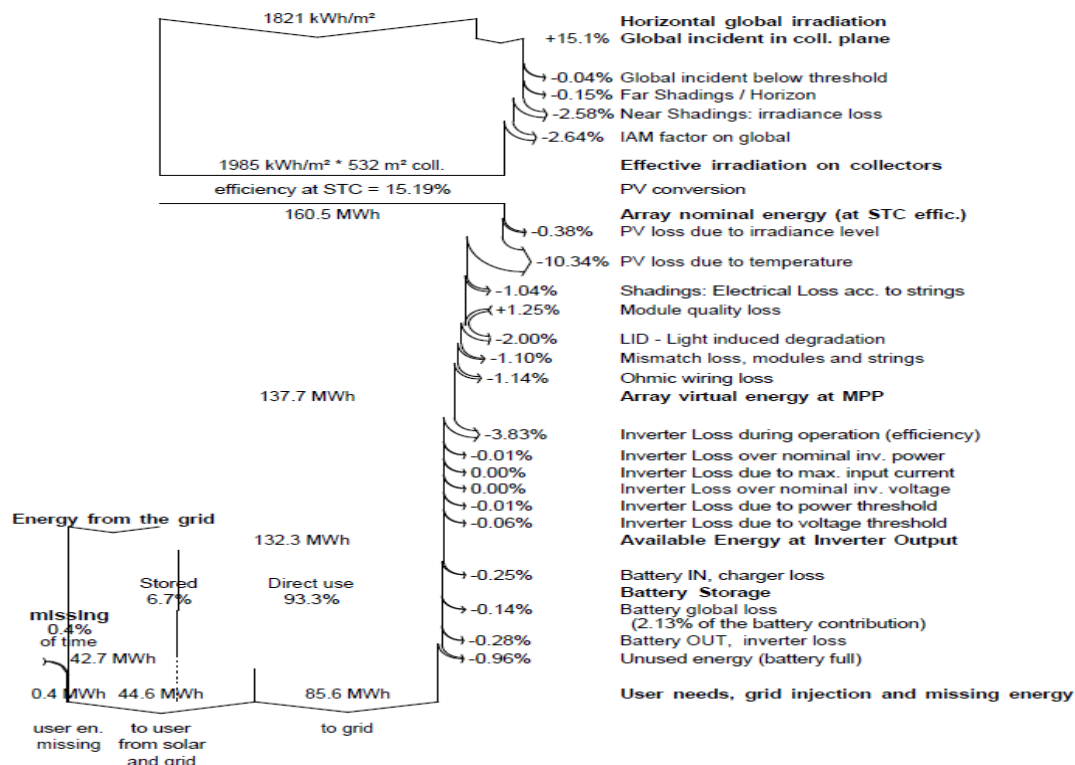
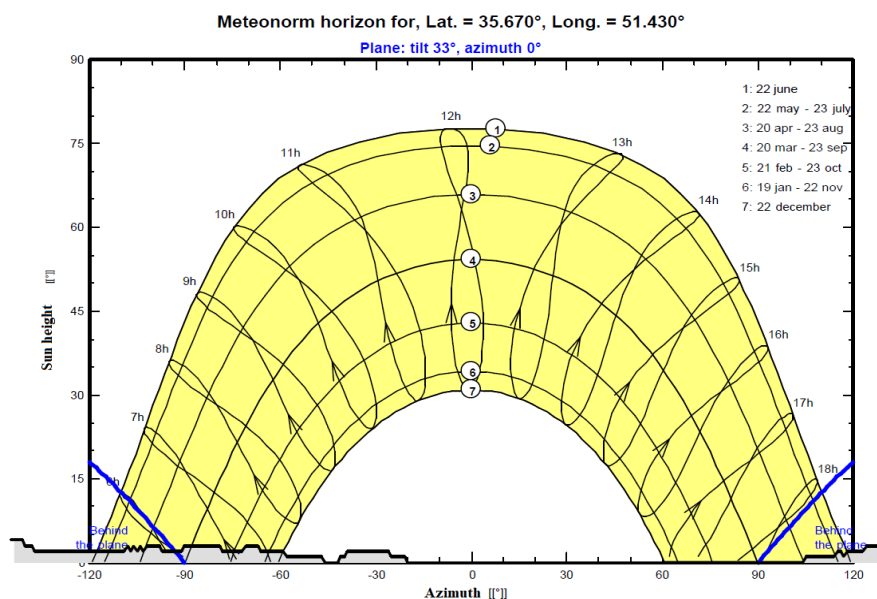**Figure 16.** Arrow loss diagram (PVsyst output)

Figure 17. Meteonorm horizon diagram for the power plant site

4.4. Economic evaluation

By considering the 20-year lifespan for the project and entering the cost specifications of the used components as well as the discount rate and annual inflation rate, Homer software can be used to calculate the model's net present cost and energy cost. Table 19 shows the results of running economic optimization in HOMER Pro software. Technical and economic data of the current system (DG (1000 kW)) versus the proposed configuration (DG (1000 kW)/PV (80 kW)/Battery) in the grid-connected mode are shown in this table.

Table 19. The technical and economic data of the current configurations

Scenario	COE[1] ($/kWh)	NPC[2] (M$)	Operating cost ($)	Grid purchased (kWh/yr)
Basic model	0.0241	3.22	150,063	248,023
Proposed system	0.0235	3.17	139,825	202,773

The information obtained in the economic evaluation of the project shows that the net present cost and cost of energy of the proposed system are lower than those of the current system. Thus, the implementation of this project is economically justified. On the other hand, operating cost and payment costs for grid electricity in the proposed configuration are 7 and 18 percent lower than those for the current system, respectively.

4.5. Environmental assessment

A summary of the emissions produced by the present system in addition to the proposed configuration is presented in Table 20. Using this configuration, carbon dioxide, carbon monoxide, Unburned Hydro Carbon (UHC), PM, and sulfur dioxide emissions decreased compared with the current system. Meanwhile, the reduction of unburned hydrocarbons (UHC) is significant, exhibiting a reduction of 17 % compared

----

[1] Cost of Energy
[2] Net Present Cost

to the base model. Information in the table proves that the deployment of the proposed model is also environmentally explainable.

Table 20. Current energy systems emission versus hybrid configuration emission

Quantity (kg/y)	Basic model	Proposed configuration
CO_2	6,348,930	6,336,802
CO	42,406	42,148
UHC	46,388	38,246
PM	198	194
SO_2	15,567	15,539
NO_x	3,950	3,865

4.6. Sensitivity analysis

Based on economic theories, there is a positive relationship between interest rate and inflation rate in many countries, and the interest rate's value reflects the inflation trend. The positive relationship between interest rate and expected inflation is a classical theory introduced by Irving Fisher and known as the Fisher effect in economic literature (Anari & Kolari, 2016).

On the other hand, the fuel price in Iran is lower than world prices due to Iran's geopolitics conditions; this leads to fuel contraband abroad and overuse of the fuel. Hence, increasing fuel prices in line with world prices is one of the government's purposes (Mukhtarov et al., 2022). On the other hand, enhancing the energy carriers' prices increases the inflation rate significantly. Consequently, enhancing fuels price (as one of the general policies of Iran) is considered along with inflation rate enhancement.

According to the above contents, a sensitivity analysis is applied to the proposed system to investigate the effect of variation in the inflation rate, discount rate, and diesel fuel price on NPC and COE.

The effects of changing the discount rate, inflation rate, and fuel price on the COE and NPC of the system are shown in Figure 18. The cost of diesel fuel is considered to vary between 0.1 $/L and 0.4 $/L, while the discount rate varies between 16 % and 20 %, and the inflation rate fluctuates between 13 and 17 percent. According to the results, by

growing the discount rate and fuel cost, the COE of the system increases. The minimum value of COE (0.0240 $/kWh) occurs when the cost of diesel is 0.1 $/L, the discount rate is 16 %, and the inflation rate is 13 %. On the other hand, the highest value of COE (0.102 $/kWh) is related to the 0.4 $/L diesel price, 20 % discount rate, and 17 % inflation rate.
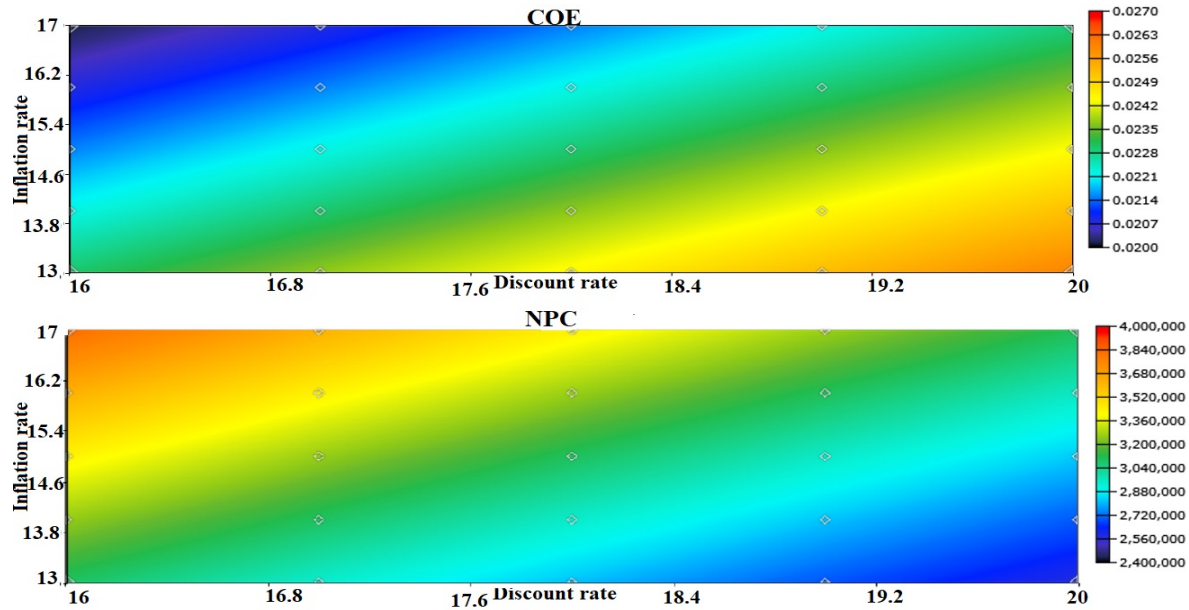

Figure 18. Effect of nominal discount and inflation rate on NPC and COE of the system

The current cost of diesel in Iran is stated as 0.1 $/L. Therefore, by considering this cost as constant, the discount rate is raised by 4 % the COE growth is 14 % (Figure 19-Plot A). On the other hand, increasing the diesel price leads to the reduction of CO_2 emission and increase of renewable fraction because the higher price of diesel fuel causes less usage of diesel generator and switching to renewable resources. Figure

19-Plot B indicates a direct relationsheep between increasing the expected inflation rate and NPC growth. As seen in Figure 19-Plot C, the COE of the system is increased by growing the diesel fuel price from 0.1 $/L to 0.2 $/L, but an increase to more than this value has minor effect on the system because photovoltaic power compensates for less diesel generator production.
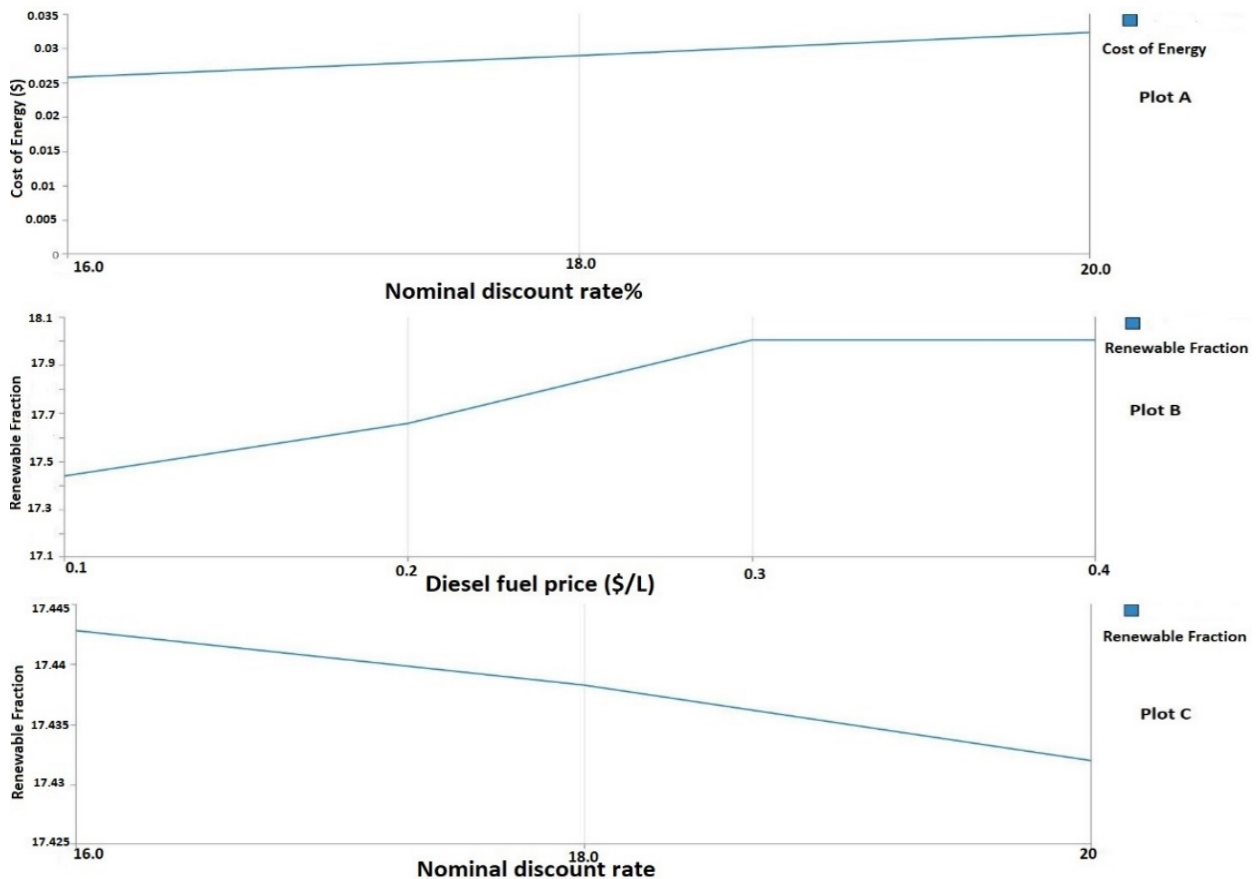

Figure 19. Linear diagram of a variation of A) COE by growing nominal discount rate; B) NPC by increasing expected inflation rate; C) COE by raising diesel fuel price

5. CONCLUSIONS

The hospital energy system was modeled with detailed information as a large-scale and complex structure in this investigation. The case study was a large hospital located in the southwest of Tehran, and the energy system of this hospital was modeled with Design-Builder software. Then, the obtained results were validated with accurate information on the hospital's energy consumption based on energy bills. In the next step, a small solar power generation unit was designed on the hospital's rooftop with the possibility of selling surplus power to the grid using PVsyst software. Design parameters such as module orientation, near shading, and inter-row spacing were evaluated. Then, the economic feasibility study of the proposed system was done using HOMER Pro software. Environmental evaluation and sensitivity analysis were also applied to the hybrid model. Finally, the project's feasibility was technically, economically, and environmentally proven. This study's most important results are summarized as follows:

- The annual electricity demand of the hospital is 3.08 GWh.

- The power plant can generate 132 MWh of solar electricity annually.

- This system can inject 85.6 MWh of its annual power into the grid.

- The net present cost of the proposed model was calculated to be 3.17 million dollars, while the cost of energy of the system was 0.0235 $/kWh.

- Growing the discount rate and fuel cost led to an increase in the COE of the system (the discount rate is raised by 4 % and the COE growth is 14 %).

The study revealed that a hybrid renewable energy system was an appropriate choice for hospitals and health centers. It is concluded from the results that renewable energies represent a valuable tool for improving the quality of power supply in hospitals. The attained results of this study can be simplified to other health centers and hospitals worldwide with each climate and weather. Applying renewable energy systems to welfare areas such as hospitals can incentivize the community to use new renewable technologies instead of traditional ones. From this research, it can be determined that hybrid renewable energy systems can compensate for the weakness of diesel generators as backup power supply and improve the total reliability of the power system, in addition to its role in reducing total emissions.

6. ACKNOWLEDGEMENT

NOMENCLATURE

Cp	Zone air specific heat (kJ/kg.K)
CT	Sensible heat capacity multiplier
h	Convective heat transfer coefficient (kW/m^2.K)
A	Surface (m^2)
T	Temperature (K)
Q	Internal load (kW)
m	Mass rate (kg/s)
q	Conduction heat flow (kW)
q″	q/A: conduction heat flux (kW/m^2)
CTF	Conduction Transfer Function
nz	Number of zones
X_j	Outside CTF coefficient, j= 0, 1, nz
Y_j	Cross CTF coefficient, j= 0, 1, nz
Z_j	Inside CTF coefficient, j= 0, 1, nz
NPC	Net Present Cost ($)
COE	Cost of Energy ($/kWh)
CT	Total annualized cost ($/year)
i	Interest rate (%)
CRF	Capital Recovery Factor
Cap	The initial capital cost of a component ($)
Cacao	The annualized capital cost of each component ($)
n	Lifetime of the project (year)
m	Number of all devices in the system
COM,	Annual operation and maintenance (O&M) cost ($/year)
Cf	Total annual fuel cost ($/year)
CR	Annualized replacement cost ($/year)
CO_2	Carbon Dioxide
CO	Carbon Monoxide
UHC	Unburned Hydrocarbons
NO_X	Nitrogen Oxides
SO_2	Sulfur Dioxide
PM	Particulate Matter
PR	Performance ratio

Greek letters

ρ	Density (kg/m^3)
δ	Time step
Φ_j	Flux CTF coefficient, j = 0, 1, nz

Subscript

j	Number of system's components

REFERENCES

1. Jahangir, M.H., Eslamnezhad, S., Mousavi, S.A. and Askari, M., "Multi-year sensitivity evaluation to supply prime and deferrable loads for hospital application using hybrid renewable energy systems", *Journal of Building Engineering*, Vol. 40, No. April, (2021), 102733. (https://doi.org/10.1016/j.jobe.2021.102733).

2. Morgenstern, P., Li, M., Raslan, R., Ruyssevelt, P. and Wright, A., "Benchmarking acute hospitals: Composite electricity targets based on departmental consumption intensities?", *Energy and Buildings*, Vol. 118, (2016), 277-290. (https://doi.org/10.1016/j.enbuild.2016.02.052).

3. Wang, T., Li, X., Liao, P.-C. and Fang, D., "Building energy efficiency for public hospitals and healthcare facilities in China: Barriers and drivers", *Energy*, Vol. 103, (2016), 588-597. (https://doi.org/10.1016/j.energy.2016.03.039).

4. García-Sanz-Calcedo, J., "Analysis on energy efficiency in healthcare buildings", *Journal of Healthcare Engineering*, Vol. 5, No. 3, (2014), 361-374. (https://doi.org/10.1260/2040-2295.5.3.361).

5. Ascione, F., Bianco, N., De Stasio, C., Mauro, G. and Vanoli, G., "Multi-stage and multi-objective optimization for energy retrofitting a developed hospital reference building: A new approach to assess cost-optimality", *Applied Energy*, Vol. 174, (2016), 37-68. (https://doi.org/10.1016/j.apenergy.2016.04.078).

6. Paksoy, H., Andersson, O., Abaci, S., Evliya, H. and Turgut, B., "Heating and cooling of a hospital using solar energy coupled with seasonal thermal energy storage in an aquifer", *Renewable Energy*, Vol. 19, No. 1-2, (2000), 117-122. (https://doi.org/10.1016/S0960-1481(99)00060-9).

7. Santika, W.G,. Urmee, T., Simsek, Y., Bahri, P.A. and Anisuzzaman, M., "An assessment of energy policy impacts on achieving Sustainable Development Goal 7 in Indonesia", *Energy for Sustainable Development*, Vol. 59. (2020), 33-48. (https://doi.org/10.1016/j.esd.2020.08.011).

8. Tamir, K., Urmee, T. and Pryor, T., "Issues of small scale renewable energy systems installed in rural Soum centers in Mongolia", *Energy for Sustainable Development*, Vol. 27. (2015), 1-9. (https://doi.org/10.1016/j.esd.2015.04.002).

9. Isa, N.M., Das, H.S., Tan, C.W., Yatim, A.H.M. and Lau, K.M., "A techno-economic assessment of a combined heat and power photovoltaic/fuel cell/battery energy system in Malaysia hospital", *Energy*, Vol. 112, (2016). (https://doi.org/10.1016/j.energy.2016.06.056).

10. Biglia, A., Caredda, F.V., Fabrizio, E., Filippi, M. and Mandas, N., "Technical-economic feasibility of CHP systems in large hospitals

through the Energy Hub method: The case of Cagliari AOB", *Energy Building*, Vol. 147, (2017), 101-112. (https://doi.org/10.1016/j.enbuild.2017.04.047).

11. Lagrange, A., de Simón-Martín, M., González-Martínez, A., Bracco, S. and Rosales-Asensio, E., "Sustainable microgrids with energy storage as a means to increase power resilience in critical facilities: An application to a hospital", *International Journal of Electrical Power and Energy Systems*, Vol. 119, No. August (2019), (2020), 105865. (https://doi.org/10.1016/j.ijepes.2020.105865).

12. Dursun, S., Aykut, E. and Dursun, B., "Assessment of optimum renewable energy system for the Somalia–Turkish training and research hospital in Mogadishu", *Journal or Renewable Energy and Environment (JREE)*, Vol. 8, No. 3, (2021), 54-67. (https://doi.org/10.30501/jree.2021.245232.1140).

13. Vaziri, S.M., Rezaee, B. and Monirian, M.A., "Utilizing renewable energy sources efficiently in hospitals using demand dispatch", *Renewable Energy*, Vol. 151, (2020), 551-562. (https://doi.org/10.1016/j.renene.2019.11.053).

14. Franco, A, Shaker, M., Kalubi, D. and Hostettler, S., "A review of sustainable energy access and technologies for healthcare facilities in the Global South", *Sustainable Energy Technologies and Assessments*, Vol. 22, (2017). (https://doi.org/10.1016/j.seta.2017.02.022).

15. Jahangir, M.H., Mousavi, S.A. and Vaziri Rad, M.A., "A techno-economic comparison of a photovoltaic/thermal organic Rankine cycle with several renewable hybrid systems for a residential area in Rayen, Iran", *Energy Conversation and Management*, Vol. 195, (2019), 244-261. (https://doi.org/10.1016/j.enconman.2019.05.010).

16. EnergyPlus, "The board of US Department of Energy (DOE), October 1, (2013)", *EnergyPlus Eng. Ref.*, (2016).

17. Rezaei, M., Boushehri, A. and Bagheri Moghaddam, N., "Factors affecting photovoltaic technology application in decentralized electricity", *Journal or Renewable Energy and Environment (JREE)*, Vol. 5, No. 3, (2018), 27-41. (https://doi.org/10.30501/jree.2018.93451).

18. Firouzjah, K.G., "Assessment of small-scale solar PV systems in Iran: Regions priority, potentials, and financial feasibility", *Renewable and Sustainable Energy Reviews*, Vol. 94. (2018), 267-274. (https://doi.org/10.1016/j.rser.2018.06.002).

19. "Shading Analysis", (2022). (https://www.pvresources.com/en/siteanalysis/shadinganalysis).

20. Kasaeian, A., Rahdan, P., Vaziri Rad, M.A. and Yan, W.M., "Optimal design and technical analysis of a grid-connected hybrid photovoltaic/diesel/biogas under different economic conditions: A case study", *Energy Conversion and Management*, Vol. 198, (2019), 111810. (https://doi.org/10.1016/j.enconman.2019.111810).

21. Mousavi, S.A., Zarchi, R.A., Astaraei, F.R., Ghasempour, R. and Khaninezhad, F.M., "Decision-making between renewable energy configurations and grid extension to simultaneously supply electrical power and fresh water in remote villages for five different climate zones", *Journal of Cleaner Production*, Vol. 279, (2021), 12361. (https://doi.org/10.1016/j.jclepro.2020.123617).

22. Hafez, O. and Bhattacharya, K.,"Optimal planning and design of a renewable energy-based supply system for microgrids", *Renewable Energy*, Vol. 45, (2012), 7-15. (https://doi.org/10.1016/j.renene.2012.01.087).

23. Haghighat Mamaghani, A., Avella Escandon, S.A., Najafi, B., Shirazi, A. and Rinaldi, F., "Techno-economic feasibility of photovoltaic, wind, diesel and hybrid electrification systems for off-grid rural electrification in Colombia", *Renewable Energy*, Vol. 97, (2016), 293-305. (https://doi.org/10.1016/j.renene.2016.05.086).